RAPID COMMUNICATIONS

PHYSICAL REVIEW B VOLUME 49, NUMBER 12 15 MARCH 1994-II

Weak localization and electron-electron interactions in a two-dimensional grid lateral surface superlattice

C.-T. Liang, C. G. Smith, J. T. Nicholls, R. J. F. Hughes, M. Pepper,* J. E. F. Frost, D. A. Ritchie, M. P. Grimshaw, and G. A. C. Jones

Cavendish Laboratory, Madingley Road, Cambridge CB3 0HE, United Kingdom

(Received 21 December 1993)

Low-field magnetoresistance measurements were performed on a two-dimensional grid lateral surface superlattice (LSSL) fabricated on a GaAs/$Al_xGa_{1-x}As$ heterojunction. From a one-parameter fit to the two-dimensional weak-localization theory we have obtained the effective inelastic scattering length at different temperatures. By subtracting the weak-localization term, we have also investigated the electron-electron interactions in this system. Both localization and interaction effects saturate at low temperatures when the inelastic scattering length and thermal diffusion length are longer than the period of the LSSL. At higher temperatures, when the thermal diffusion length becomes comparable to the period of the LSSL, the electron-electron interaction term causes the conductivity to decrease logarithmically with temperature. These results can be explained in terms of coherent backscattering of the electrons in a fraction of the electron puddles formed below the superlattice gate. Disorder ensures that the cells showing these results are not neighbors, so that this effect is an ensemble average of many unit cells several periods apart.

Esaki and Tsu[1] suggested that by defining a periodic potential longer than that of the atomic lattice it should be possible to observe Bragg reflection of transport electrons, giving rise to negative differential resistance (NDR); recently Bloch oscillations have been observed[2] in a periodic vertical tunneling structure. The two-dimensional (2D) equivalent of such a device can be realized by patterning a lateral surface superlattice (LSSL) gate above a two-dimensional electron gas (2DEG) formed at the interface of a GaAs/$Al_xGa_{1-x}As$ heterostructure. The amplitude of the periodic potential can be tuned by varying the voltage applied to the superlattice gate. In antidot arrays, where the electrons are depleted under the LSSL, the quenching of the Hall effect,[3] single[3] and double[4] frequency Aharonov-Bohm oscillations in low magnetic fields and Coulomb blockade near pinch-off[5] have been observed. Besides the possibility of observing NDR, the prediction of Landau-level splitting and the possibility of observing the "Hofstadter butterfly"[6] whenever the flux quanta per unit cell is a rational fraction of the magnetic field has attracted much attention to the 2D grid LSSL. Such devices have been fabricated on GaAs/$Al_xGa_{1-x}As$ heterostructures and many new phenomena have been observed.[7-10]

Using an optical interference method Weiss *et al.*[11] introduced a weak submicrometer periodic potential and discovered magnetoresistance oscillations periodic in $1/B$. The extrema in magnetoresistance are observed when the cyclotron radius is commensurate with the superlattice period of the LSSL.[12] Paris *et al.*[10] measured weak localization in a 2D grid LSSL and Gao *et al.*[13] investigated the effect of a one-dimensional LSSL on weak localization in silicon inversion layers and obtained qualitative agreement with a recent theory[14] invoking an anisotropic diffusion constant. However, weak localization and electron-electron interactions in a 2DEG system under a 2D periodic potential have not been investigated as a function of temperature, and it is the purpose of this paper to report such measurements.

There are two distinct theories that explain the logarithmic dependence of conductivity with temperature observed[15] in weakly disordered 2D electron systems: weak-localization theory and electron-electron interaction theory.[16] Although both theories predict the same temperature dependence of the conductivity, the two effects can be distinguished by low-field magnetoresistance measurements in a perpendicular magnetic field.[17] The weak-localization contribution to the magnetoconductivity of a disordered 2D system is given by[18]

$$\sigma_{xx}(B)-\sigma_{xx}(0)=\left[\frac{e^2}{2\pi^2\hbar}\right]\left\{\psi\left[\frac{1}{2}+\frac{\hbar}{4eBl_{\rm eff}^2}\right]-\psi\left[\frac{1}{2}+\frac{\hbar}{2eBl^2}\right]+\ln\left[2\frac{l_{\rm eff}^2}{l^2}\right]\right\}, \quad (1)$$

where ψ is the digamma function. $l_{\rm eff}$ is the effective inelastic scattering length to be discussed later, and l is the elastic scattering length. At zero magnetic field, the correction term due to weak localization is[19]

$$\delta\sigma(0)=(e^2/2\pi^2\hbar)\ln(2l_{\rm eff}^2/l^2+1)\ . \quad (2)$$

At low temperatures, when electron-electron scattering is the phase-breaking mechanism, $1/\tau_\phi$ in 2D is given by[20]

$$1/\tau_\phi=(kT/2\pi N_0 D\hbar^2)\ln(\pi D N_0\hbar),\quad T<\hbar/k\tau\ , \quad (3)$$

where N_0 is the 2D density of states, D is the diffusion

constant. τ and τ_ϕ are elastic scattering and phase-breaking time, respectively.

When considering the electron-electron interactions at finite temperature T, the time $\tau_T \equiv \hbar/kT$ enters as a long-time cutoff,[21] and is equivalent to using the thermal diffusion length $l_T = \sqrt{D\tau_T}$ as the cutoff length scale. The correction term due to the electron-electron interactions in a 2D system is given by[16]

$$\delta\sigma = (e^2/4\pi^2\hbar)(2 - \tfrac{3}{2}\tilde{F})\ln kT\tau/\hbar \,, \tag{4}$$

where

$$\tilde{F} = -4[1 - 2(1+F/2)\ln(1+F/2)/F] \,. \tag{5}$$

The Thomas-Fermi screening factor F is given by[16]

$$F = (1/\sqrt{1-x^2})[1 - (2/\pi)\tan^{-1}(x/\sqrt{1-x^2})] \,, \tag{6}$$

where $x = 2k_F/K$, k_F is the Fermi wave vector, $K = e^2 N_0/2\varepsilon\varepsilon_0$, and $\varepsilon = 13.1$ for GaAs.

The theories described above are valid for infinite systems. Kaveh *et al.*[22] proposed that when the length L and width w of a device become comparable to the theoretical inelastic scattering length l_ϕ, finite-size effects occur and the effective inelastic scattering length l_{eff} is given by

$$1/l_{\text{eff}}^2 = 1/l_\phi^2 + 1/L^2 \,. \tag{7}$$

Similarly, Choi, Tsui, and Palmateer[23] suggested that for interaction effects the effective thermal diffusion length $l_{T_{\text{eff}}}$ is given by $1/l_{T_{\text{eff}}} = 1/l_T + \alpha/L$, where α is a constant dependent on the boundary conditions.

The grid superlattice gate device (0.3-μm period and 0.08-μm linewidth) shown in Fig. 1(a) was defined by electron beam lithography on the surface of a $GaAs/Al_xGa_{1-x}As$ heterostructure, 70 nm above the 2DEG, with Au/Ti evaporation and subsequent lift-off. To observe weak localization in this system, we applied a negative voltage of -0.31 V to the gate to reduce the electron concentration beneath the grid gates; however, in the puddles between the gates the electron concentration should be slightly reduced. The carrier concentration under the grid gates is 8.34×10^{10} cm^{-2} and the estimated mobility is 2.28×10^4 cm^{2}V^{-1}s^{-1}, assuming the conductivity is uniform over the entire device. The corresponding elastic scattering length l is 0.1 μm. Note that the product $k_F l = 7.24$, indicating that the sample is in the weak-localization regime. Experiments were performed over a temperature range of 0.05–0.85 K in a dilution refrigerator and at 2.4 K. The magnetoresistance was measured using standard four-terminal ac phase-sensitive techniques. The weak-localization effects were not sensitive to the driving current varying between 1 and 10 nA, and when a gate voltage of -0.35 V was applied to the grid, there was a large background change in resistance on going from 0.05 to 0.34 K. Both these observations imply that there was very little electron heating over the range of our measurements.

We have observed the negative magnetoresistance at low magnetic fields and subsequent Weiss oscillations at ±0.18 T. We also observed a slight quench of the Hall effect at low magnetic fields, indicating that our system is not a perfect grid potential but is a "grid plus antidot" potential. The antidotlike potential is created in the region where the grids cross one another. Figure 2 shows the suppression of the weak localization in a perpendicular magnetic field at different temperatures. The raw data were inverted to get the magnetoconductivities. When the temperature was raised, the weak-localization effects were gradually suppressed on going from 0.05 to 0.85 K and were not observable at 2.4 K. From fits of the experimental data to Eq. (1) we obtain the effective inelastic scattering length l_{eff}. The theoretical conductivities are shown as solid lines in Fig. 2, and the corresponding $l_{\text{eff}}(T)$ is shown in Fig. 3(a). The zero-field conductivity consists of three parts: a classical Drude conductivity, a weak-localization contribution, and a correction term due to electron-electron interactions. Figure 3 shows that the conductivity saturates below 0.44 K where $\ln T = -0.82$, and exhibits a $\ln T$ dependence at higher temperatures.

In our system the diffusion constant $D = 67.3$ cm^{2}s^{-1} is dominated by the regions under the grid gates. The elastic scattering time $\tau = 8.84\times10^{-13}$ s and $\hbar/k\tau = 8.6$ K. According to Eq. (3), $1/\tau_\phi \to 0$, as $T \to 0$, leading to an infinite inelastic scattering length at $T = 0$ K. Using

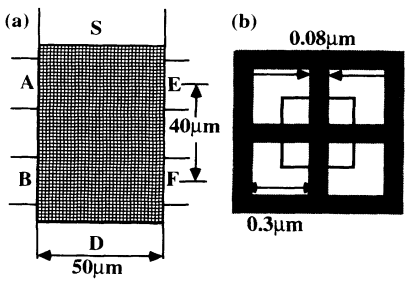

FIG. 1. (a) The configuration of the device; A, B, E, and F are voltage probes. S and D are source and drain contacts. (b) A closeup of a 0.3×0.3 μm^2 unit cell of the superlattice. The shaded area corresponds to the superlattice gate.

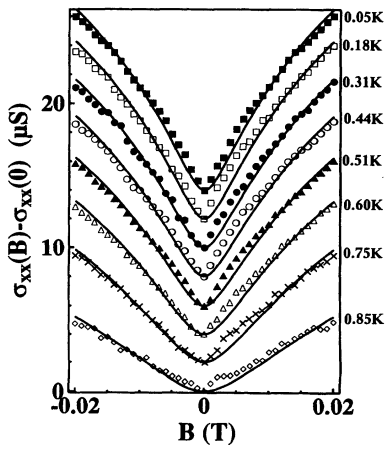

FIG. 2. The magnetoconductivity $\sigma_{xx}(B) - \sigma_{xx}(0)$ at different temperatures. Each curve has been vertically offset for clarity. The solid curves are the theoretical fits to Eq. (1).

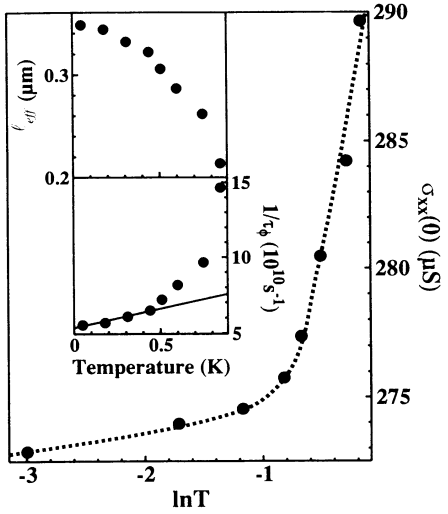

FIG. 3. The zero-field conductivity $\sigma_{xx}(0)$ vs $\ln T$. The dotted line is a guide to the eye. Inset: (a) The fitting parameter $l_{\rm eff}$ and (b) phase-breaking rate $1/\tau_\phi$, vs temperature. The straight line fit is discussed in the text.

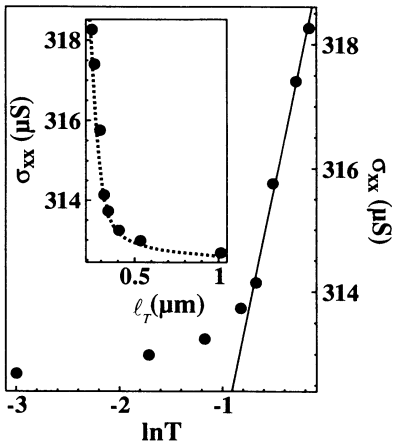

FIG. 4. The zero-field conductivity σ_{xx} vs $\ln T$, after subtraction of the weak-localization term. The straight line fit is discussed in the text. The inset shows σ_{xx} as a function of thermal diffusion length l_T. The dotted line is a guide to the eye.

the relation $l_{\rm eff}=\sqrt{D\tau_\phi}$ we have determined $1/\tau_\phi$ as a function of temperature from $l_{\rm eff}(T)$, the results are plotted in Fig. 3(b). There is a good fit to $1/\tau_\phi=(2.478\times10^{10}T+5.353\times10^{10})$ s^{-1} for the lowest four temperatures: 0.05, 0.18, 0.31, and 0.44 K. Surprisingly, the fit shows a temperature-independent term. The term that is linear in T is close to that predicted from Eq. (3); the temperature-independent term corresponds to a length of 0.355 μm, close to the period of the LSSL. It is noted that Newson *et al.*[24] also observed a similar behavior of $1/\tau_\phi=AT^{3/2}+B$ for 3D weak localization in $In_xGa_{1-x}As$ devices; the saturation in $l_{\rm eff}$ occurred when $l_{\rm eff}$ was comparable to the average separation of In-rich clusters.

According to Eq. (2), we can calculate the weak-localization contribution to the conductivity at zero magnetic field from $l_{\rm eff}(T)$. Only the electron-electron interaction term and the classical Drude conductivity remain after subtraction of the weak-localization term. At low temperatures, the classical term is temperature independent; therefore we can investigate the electron-electron interactions at different temperatures. As shown in the inset to Fig. 4, our data qualitatively agree with the saturation of the interaction effects[23] at low temperatures where the thermal diffusion length is longer than the period of the LSSL. From the slope of the high-temperature conductivity in Fig. 4 we determine $\tilde{F}=0.47$, this is in reasonable agreement with the value $\tilde{F}=0.63$ calculated from the carrier concentration under the grid gates using Eqs. (5) and (6).

In the superlattice device we are measuring many small devices with a 0.3×0.3 μm^2 unit cell, arranged in both parallel and in series. The absence of conductance fluctuations[25] shows that one small area does not dominate the conductance, and that we are measuring the ensemble average of many devices. Using Eq. (7) to fit the low-temperature $l_{\rm eff}(T)$ we deduce $L=0.354$ μm, close to the period of the superlattice.

We now consider possible explanations for the saturation of the localization and interaction effects. The first is that under all the grid gates the electron mobility has been reduced to such an extent that the motion is diffusive, but still ballistic in the puddles. If this is the case we are measuring the averaged localization effects of many short narrow barrier regions in a periodic array. The result would then imply that whenever the electrons pass through the puddles they undergo an inelastic scattering process thereby saturating the effective inelastic scattering length. However, this does not explain the saturation of the interaction effects.

A more plausible explanation relies on the fact that elastic scattering length $l=0.1$ μm, is comparable to the grid width, implying that disorder serves only to modify the barrier heights and widths under the grid gates, but does not lead to diffusive transport in those regions. In this case each unit square looks like a 0D quantum dot.[26] If we assume the transport is ballistic above the barriers, the conductivity of the device shows that there are four subbands above the barriers in each unit cell. The carrier concentration under the grid gate also corresponds to there being four half Fermi wavelengths between the anti-dot regions where the grid lines cross. For a single puddle, quasilocalization of electrons above the puddle is observed when an exact number of half Fermi wavelengths fit between the barriers. When the temperature is raised the localization disappears when the inelastic scattering length becomes shorter than the puddle size. In a single quantum dot this effect occurs only when the barrier heights are identical. The quasilocalization results from the coherent backscattering of the electrons between the two barriers.[27] The existence of disorder under the grid gates ensures that the matching condition does not occur in neighboring puddles. Thus the measured localization and interaction effects are quasi-0D in nature and suggest that if we could make our puddles identical to form a dot lattice then we would observe minibands instead. To our

knowledge, there is no theory concerning weak localization in a 2D periodic potential and the anisotropic diffusion constant argument[17] cannot be applied to our case. Although we have a good fit to the 2D weak-localization theory, whether the theory is applicable to our system is an open question.

In conclusion, we have investigated the weak-localization and electron-electron interactions in a 2D grid LSSL. Both localization and interaction effects saturate at low temperatures when the inelastic scattering length and thermal diffusion length are longer than the period of the LSSL. These results can be explained in terms of coherent backscattering of the electrons in a fraction of the puddles formed below the superlattice gate. Disorder ensures that the cells showing these results are not neighbors, so that this effect is an ensemble average of many unit cells several periods apart.

This work was funded by the Science and Engineering Research Council. We thank Professor D. E. Khmelnitskii and Professor M. Kaveh for useful discussions. C.T.L. acknowledges support from the Committee of Vice-Chancellors and Principals, UK.

---

*Also at Toshiba Cambridge Research Centre, 260 Cambridge Science Park, Milton Road, Cambridge CB4 4WE, United Kingdom.

[1]L. Esaki and R. Tsu, IBM J. Res. Dev. **14**, 61 (1970).
[2]C. Waschke *et al.*, Phys. Rev. Lett. **70**, 3319 (1993).
[3]C. G. Smith *et al.*, J. Phys. Condens. Matter **2**, 3405 (1990).
[4]G. M. Gusev *et al.*, J. Phys. Condens. Matter **4**, L269 (1992).
[5]C. G. Smith *et al.*, J. Vac. Sci. Technol. B **10**, 2904 (1992).
[6]D. R. Hofstadter, Phys. Rev. B **14**, 2239 (1976).
[7]G. Bernstein and D. K. Ferry, J. Vac. Sci. Technol. B **5**, 964 (1987).
[8]K. Ismail *et al.*, Appl. Phys. Lett. **54**, 460 (1989).
[9]K. Ismail *et al.*, Appl. Phys. Lett. **55**, 2766 (1989).
[10]E. Paris *et al.*, J. Phys. Condens. Matter **3**, 6605 (1991); in *Nanostructures and Mesoscopic Systems*, edited by W. P. Kirk and M. A. Reed (Academic, New York, 1991), p. 311.
[11]D. Weiss *et al.*, Europhys. Lett. **8**, 179 (1989).
[12]R. R. Gerhardts, D. Weiss, and K. von Klitzing, Phys. Rev. Lett. **62**, 1173 (1989); C. W. J. Beenakker, *ibid.* **62**, 2020 (1989).
[13]J. R. Gao *et al.*, Phys. Rev. B **46**, 9885 (1992).
[14]W. Szott, C. Jedrzejek, and W. P. Kirk, Superlatt. Microstruct. **11**, 199 (1992).
[15]M. J. Uren, R. A. Davies, and M. Pepper, J. Phys. C **13**, L985 (1980).
[16]For a review, see B. L. Al'tshuler and A. G. Aronov, in *Electron-Electron Interactions in Disordered Systems*, edited by A. L. Efros and M. Pollak (North-Holland, Amsterdam, 1985), p. 1; H. Fukuyama, *ibid.*, p. 155; P. A. Lee and T. V. Ramakrishnan, Rev. Mod. Phys. **57**, 287 (1985), and references therein.
[17]R. A. Davies, M. J. Uren, and M. Pepper, J. Phys. C **14**, L531 (1981); D. A. Poole, M. Pepper, and R. W. Glew, *ibid.* **14**, L995 (1981).
[18]B. L. Al'tshuler *et al.*, Phys. Rev. B **22**, 5142 (1980).
[19]C. W. J. Beenakker and H. van Houten, Phys. Rev. B **38**, 3232 (1988).
[20]B. L. Al'tshuler, A. G. Aronov, and D. E. Khmelnitskii, J. Phys. C **15**, 7367 (1982); H. Fukuyama and E. Abrahams, Phys. Rev. B **27**, 5976 (1983).
[21]G. Bergmann, Phys. Rev. B **35**, 4205 (1987).
[22]M. Kaveh *et al.*, J. Phys. C **14**, L413 (1981).
[23]K. K. Choi, D. C. Tsui, and S. C. Palmateer, Phys. Rev. B **33**, 8216 (1986).
[24]D. J. Newson *et al.*, J. Phys. C **18**, L1041 (1985).
[25]B. L. Al'tshuler, Pis'ma Zh. Eksp. Teor. Fiz. **41**, 530 (1985) [JETP Lett. **41**, 648 (1985)]; P. A. Lee and A. D. Stone, Phys. Rev. Lett. **55**, 1622 (1985).
[26]C. G. Smith *et al.*, J. Phys. C **21**, L893 (1988).
[27]L. Martin-Moreno and C. G. Smith, J. Phys. Condens. Matter **1**, 5421 (1989).

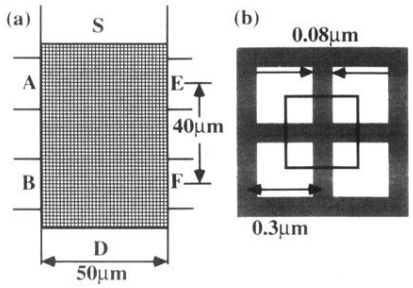

FIG. 1. (a) The configuration of the device; *A*, *B*, *E*, and *F* are voltage probes. *S* and *D* are source and drain contacts. (b) A closeup of a 0.3×0.3 μm^2 unit cell of the superlattice. The shaded area corresponds to the superlattice gate.